

SOURCES OF OSCILLATION FREQUENCY INCREASE WITH RISING SOLAR ACTIVITY

W. A. DZIEMBOWSKI

Warsaw University Observatory and Copernicus Astronomical Center, Al. Ujazdowskie 4, 00478 Warsaw, Poland

AND

P. R. GOODE

Big Bear Solar Observatory, New Jersey Institute of Technology, 40386 North Shore Lane,
Big Bear City, CA 92314-9672; pgoode@bbsso.njit.edu

Received 2004 June 11; accepted 2005 February 15

ABSTRACT

We analyze and interpret *SOHO* MDI data on oscillation frequency changes between 1996 and 2004, focusing on differences between the activity minimum and maximum of solar cycle 23. We study only the behavior of the centroid frequencies, which reflect changes averaged over spherical surfaces. Both the f -mode and p -mode frequencies are correlated with general measures of the Sun's magnetic activity. However, the physics behind each of the two correlations is quite different. We show that for the f -modes the dominant cause of the frequency increase is the dynamical effect of the rising magnetic field. The relevant rise must occur in subphotospheric layers reaching to some 0.5–0.7 kG at a depth of about 5 Mm. However, the implied constraints also require the field change in the atmosphere to be so small that it has only a tiny dynamical effect on p -mode frequencies. For p -modes, the most plausible explanation of the frequency increase is a less than 2% decrease in the radial component of the turbulent velocity in the outer layers. Lower velocity implies a lower efficiency of the convective transport, hence lower temperature, which also contributes to the p -mode frequency increase.

Subject headings: Sun: activity — Sun: helioseismology — Sun: oscillations

Online material: color figures

1. INTRODUCTION

We now have data on the evolution of solar oscillation frequencies covering nearly all of solar cycle 23. Information about cycle-dependent changes in solar oscillations includes data on the mean multiplet frequencies, $\bar{\nu}_{\ell n}$, the multiplet structures described by the $a_{k, \ell n}$ coefficients, corresponding mode amplitudes, and widths. In this paper, we focus on changes in the $\bar{\nu}$.

The correlation between p -mode frequencies and the magnetic activity cycle was first observed during the declining phase of cycle 21 (Woodard & Noyes 1985) and confirmed during the next cycle by a number of independent studies (Libbrecht & Woodard 1990; Woodard et al. 1991; Bachmann & Brown 1993; Elsworth et al. 1994; Regulo et al. 1994; Chaplin et al. 1998). The increase of f -mode frequencies with rising activity was discovered during the rising phase of the current cycle.

The physical origin of oscillation frequency increases with rising activity has been a matter of controversy. The first explanation, given by Goldreich et al. (1991, hereafter GMWK), was that the dominant cause of frequency growth with activity is the effect of an averaged small-scale magnetic field changing the frequencies directly through the perturbed Lorentz force and indirectly through the induced pressure change. An objection to this explanation was raised by Kuhn (2000), who argued that direct measurements of the rms field in the Sun's photosphere (Lin 1995; Lin & Rimmele 1999) preclude the field growth required in this picture. Instead, he proposed that the main effect causing p -mode frequency rise is a decrease in turbulent velocity due to the rising field's inhibition of convection, which is believed to be the main effect of the magnetic field on the Sun's interior structure (e.g., Spruit 2000).

As for the f -modes, Antia et al. (2000) first noted that the frequency rises with rising activity and that it is roughly proportional to the frequency itself. Such behavior could be ac-

counted for by a solar radius decrease. The number quoted by these authors was 5 km during the 3 yr of the rising phase of the cycle. This result was broadly confirmed by Dziembowski et al. (2001, hereafter DGS), who analyzed *SOHO* MDI data and found that the f -mode frequency shifts may be explained by two components, one being similar to that found by Antia et al. (2000) and the other growing more rapidly with frequency. DGS pointed out that the former component cannot arise from a shrinking of the photospheric radius but rather must come from a layer located between 4 and 8 Mm beneath the photosphere. They also suggested that the shrinking is caused by an increase of the radial component of a small-scale magnetic field beneath 8 Mm below the surface having a 1–10 kG level rms value.

The result presented by DGS was criticized by Antia (2003), who argued that the f -mode signal found in *SOHO* MDI could be completely accounted for by an annual variation of a nonsolar origin. We do not agree with his criticism. However, we still regarded it useful to reconsider our interpretation, having now a much larger data set in hand. Indeed, the interpretation presented in this paper is different: we now attribute the observed rise of f -mode frequencies directly to the rise of the magnetic field in the layers sampled by f -modes—that is, the outer 8 Mm.

2. FREQUENCY CHANGES BETWEEN 1996 AND 2004 FROM *SOHO* MDI DATA

Libbrecht & Woodard (1990), who first determined activity-related p -mode frequency shift for modes over a broad range of degrees, ℓ , noted that most of the frequency dependence of the shift is described by the inverse of the mode inertia, $I_{\ell n}$, which they called mode mass. We thus express the frequency shifts in the form

$$\Delta\bar{\nu}_{\ell n} = \frac{\gamma_{\ell n}}{\bar{I}_{\ell n}}, \quad (1)$$

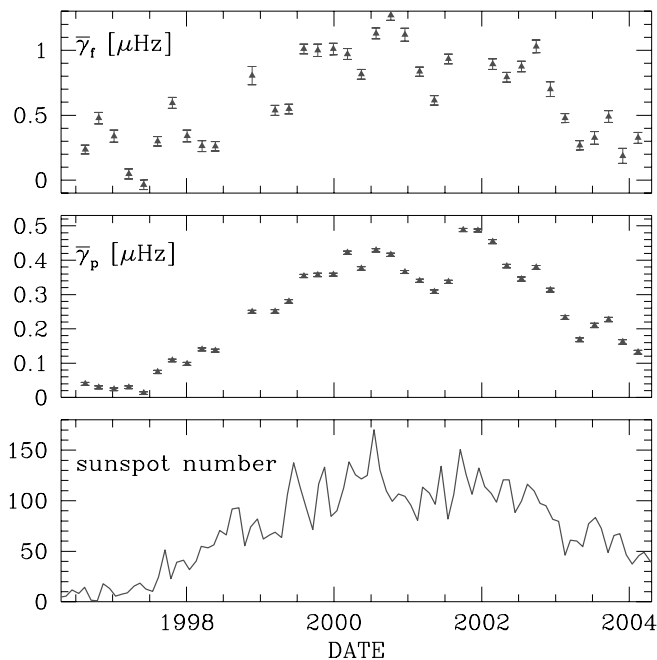


FIG. 1.—Averaged γ -values, which are the global helioseismic measure of solar activity, are derived from 38 *SOHO* MDI data sets compared with monthly sunspot numbers shown in the bottom panel. Note that the p -mode γ -values (middle) closely replicate changes in the sunspot number (bottom) and also other general measures of solar activity during the cycle. The behavior of the f -modes (top) is similar, but the values are less significant. The larger errors are mainly a consequence of the fact that the f -mode spectrum is an order of magnitude sparser. [See the electronic edition of the *Journal* for a color version of this figure.]

where $\tilde{I}_{\ell n}$ is dimensionless mode inertia, which is calculated assuming a common normalization of the radial mean displacement in the photosphere. Such calculations require a solar model. In this work, we use model S of Christensen-Dalsgaard et al. (1996). The adopted normalization is such that $\tilde{I}_{10,19} = 1$. Values of $\tilde{I}_{\ell n}$ decrease with ℓ . The n -dependence is more complicated. At low n , there is a sharp increase. The minimum inertia is reached at intermediate orders, which at $\ell = 10$ corresponds to $n = 22$ and a frequency of about 3.8 mHz. The p -mode data extend up to $\ell = 200$ and cover a frequency, ν , range of 1.1–4.5 mHz. For these latter modes, the mode dependence is essentially reduced to a simple ν -dependence (see Fig. 4 in DSG). The lack of a separate ℓ -dependence tells us that the sources of frequency shift must be localized in the outer layers above the lower turning point for the modes in the sample, or at least for the modes that matter.

We emphasize that we treat the f -modes separately, because even in the outer layers these modes have vastly different properties than those of p -modes at the same frequency. Hence, we cannot expect the same $\gamma(\nu)$ dependence for both types of modes. The kernels for calculating γ -values resulting from changes in the magnetic field, turbulent pressure, and temperature calculated by Dziembowski & Goode (2004, hereafter DG) are indeed very different for these two types of modes. In particular, for p -modes the dominant terms in the kernels are proportional to $|\nabla \cdot \xi|^2$, where ξ denotes the displacement eigenvector, while for f -modes the dominant term is $\ell|\xi|/r \gg |\nabla \cdot \xi|$. In the next section, as in DGS, we consider representations including the “radius” for f -modes, but we argue against a significant role for it. Both types of $\gamma(\nu)$ dependence are helioseismic probes of the averaged changes over spherical surfaces in the subphotospheric layers during the activity cycle. However, they are independent probes.

The plots in Figure 1 show the frequency-averaged γ -values for all available data sets from *SOHO* MDI measurements calculated from frequency differences relative to the first set from the activity minimum of cycle 23. For comparison, in the bottom panel we show the monthly sunspot number taken from the National Geophysical Data Center.¹ For the f -modes, we fit a constant (ν -independent) values for γ . For the p -modes, we fit a three-term Legendre polynomial series. We used all available frequencies in the two averaged sets. The frequency differences are weighted by the inverse of the sum of the squared errors. The similarity in the behavior of the p - and f -modes seen in the two upper panels might suggest that the source of the changes is the same in both cases, but, as we shall see, this is not true.

3. THE $\gamma(\nu)$ DEPENDENCE FOR f - AND p -MODES

The ν -dependence yields a clue to the physics of frequency change. By averaging frequencies over five sets covering nearly 1 yr of the solar minimum phase and 10 sets covering 2 yr of the maximum phase, we averaged out the annual changes that are apparently nonsolar in origin (DGS; Antia 2003). Most of the short-timescale frequency changes are a reflection of variations in solar activity, but our aim here is to explain the dominant source of the change between minimum and maximum. The price for averaging the p -mode data is a χ^2 that is about a factor of 3 larger than those for individual sets. Note in Figure 1 that the dispersion among the averaged sets is much larger than the errors.

Figure 2 shows individual $\gamma_{\ell n}$ values with the 1σ error bars and the Legendre polynomial fits. The fit depends on the truncation order, N_{tr} , of the polynomial, but the results stabilize at $N_{\text{tr}} = 3$ for the f -modes and $N_{\text{tr}} = 7$ for p -modes. The robust feature of the $\gamma(\nu)$ dependence for the f -modes is the gradual decrease of γ between $\nu = 1.37$ and 1.74 mHz, corresponding to the ℓ -range of 185–300.

Including a ΔR_f term representing variations of the f -mode radius does not lead to stable results. The radius $R_f \approx 0.99 R_{\odot}$, defined in DGS, corresponds to the bottom of the layer where all the f -modes in the data set are trapped. The numbers in Table 1 demonstrate the erratic behavior of ΔR_f and $\bar{\gamma}$ with increasing N_{tr} . Within the error bars, the result obtained with $N_{\text{tr}} = 0$ is the same as that quoted by DGS. With more terms, the fit is improved but the inferred values become meaningless. Low χ^2 and stable γ -values are obtained only after excluding the ΔR_f term. We thus abandon the idea that the rise of f -mode frequencies is caused by a shrinking of the radius beneath the bottom of the f -mode zone. With the data available in 2000, when the first interpretations of the f -mode frequency changes were given, the data did not allow for more than a two parameter fit. Furthermore, we found that averaging the frequency data taken during solar minimum and maximum sets was essential for the present inference. In § 4, we argue that the dominant part of the frequency increase is due to an in situ rise of the magnetic field.

The robust feature of the $\gamma(\nu)$ dependence for the p -modes is the steady increase beyond $\nu = 2$ mHz. We stress that the significant decreasing trend in $\gamma(\nu)$ over the 1.4–1.74 mHz frequency range found for the f -mode cannot be replicated if one looks for a common $\gamma(\nu)$ dependence for all the modes, which naturally would be dominated by the more abundant p -modes. For both p - and f -modes, higher frequency means a stronger sampling of the outermost layers. Therefore, the opposing behavior of the two types of modes at the high-frequency end of the

¹ See ftp://ftp.ngdc.noaa.gov/STP/SOLAR_DATA/SUNSPOT_NUMBERS/MONTHLY.

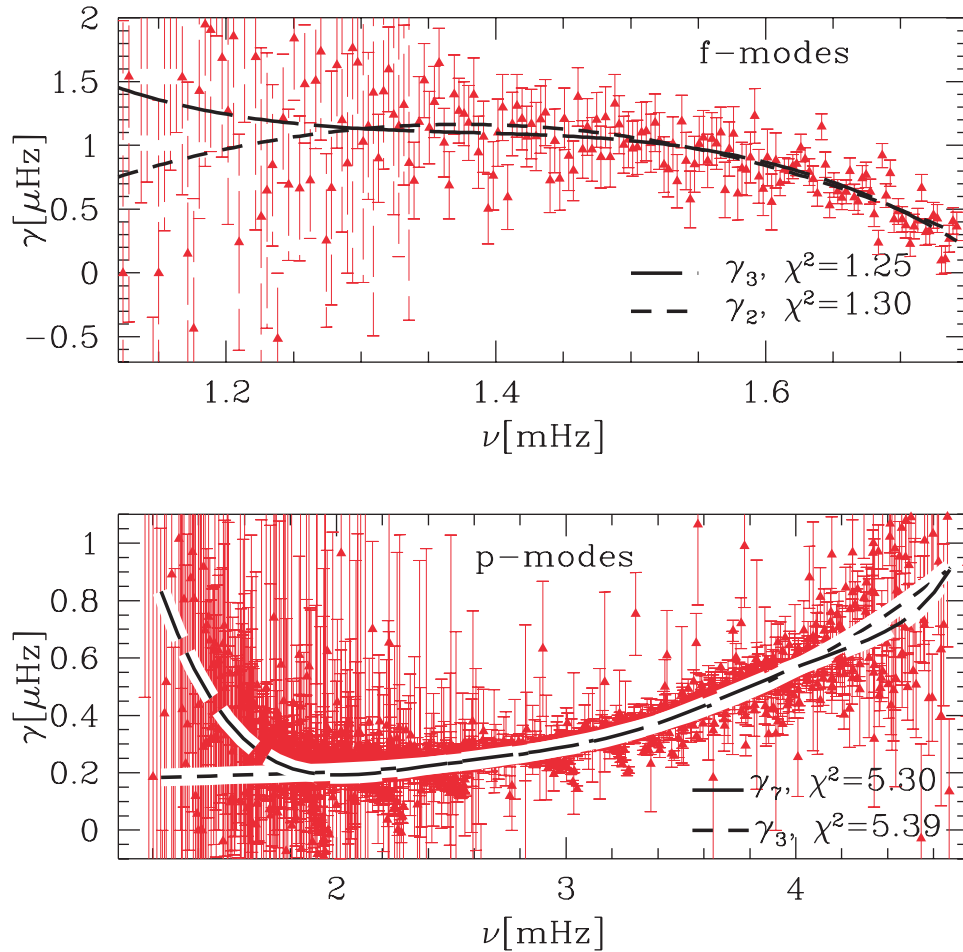


FIG. 2.—Frequency dependence of γ derived from the frequency difference between averaged frequencies from solar maximum phase (2000.4–2002.4) and minimum phase (1996.3–1997.3). The lines represent fits using truncated Legendre polynomial series. Subscripts to γ denote the order at which the series was truncated. The quoted values of χ^2 are calculated per degree of freedom.

spectrum suggests that different physical effects are responsible for the frequency increase correlated with rising solar activity.

The smallest values of χ^2 for the p -modes are significantly higher than those for the f -modes. Undoubtedly, the relatively higher χ^2 is caused by temporal fluctuations in activity during the maximum phase (for the f -modes such fluctuations are closer to being within the relatively larger error bars). However, the relatively high χ^2 for the maximum phase with respect to the minimum might also be due to an inadequacy of the fit in which the mode dependence in $\gamma_{\ell n}$ comes only through frequency. For

instance, an additional mode dependence is expected because of changes buried in the deep layers located below or near the turning of certain p -modes in the sample. To check, we plot the residuals against the position of the mode turning points, as determined by

$$f_{\ell\nu} \equiv (\ell + 0.5) \frac{1 \text{ mHz}}{\nu},$$

and show the results in Figure 3. We see that for $f_{\ell\nu} > 50$, corresponding to a turning point of depth of less than 40 Mm,

TABLE 1
FIT RESULTS

N_{tr}	ΔR_f (km)	$\bar{\gamma}$	χ^2
0.....	0	0.70 ± 0.02	3.18
1.....	0	1.19 ± 0.04	1.56
2.....	0	0.91 ± 0.06	1.30
3.....	0	1.06 ± 0.08	1.25
0.....	-4.79	0.41 ± 0.04	2.14
1.....	5.41	1.94 ± 0.15	1.39
2.....	-7.90	-0.50 ± 0.58	1.26
3.....	10.23	3.06 ± 2.60	1.26

NOTE.—Fitting the f -mode frequency shifts to $\Delta\nu = -\frac{3}{2}(\Delta R_f/R)\nu + [\gamma(\nu)/\bar{I}]$ using the Legendre polynomial series truncated at N_{tr} for $\gamma(\nu)$.

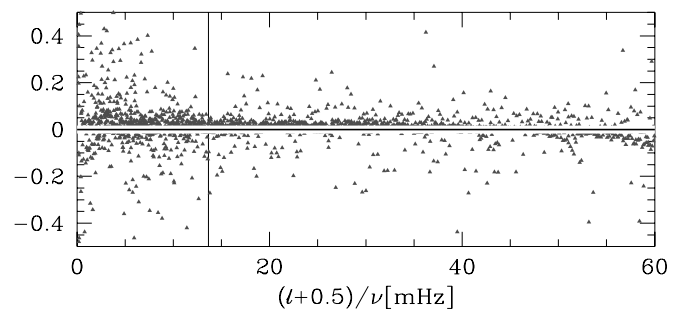


FIG. 3.—Residuals of $\gamma_{\ell n}$ for p -modes after removing the $\gamma_{\gamma}(\nu)$ fit (see Fig. 2) plotted against position of the lower turning point. The value $(\ell + 0.5)/\nu = 50$ corresponds to a depth of 40 Mm. The vertical line indicates the bottom of the convective envelope. [See the electronic edition of the *Journal* for a color version of this figure.]

the residuals are on average somewhat less than zero, while they are greater than zero for $f_{\ell\nu} < 50$. This means that a detectable contribution to the p -mode frequency changes arises in the layers reaching down to a depth of 40 Mm. However, most of the contribution arises in much shallower layers. Note that there is no visible contribution from the vicinity of the bottom of the convective envelope.

There are various potential contributors to the frequency changes described by the $\gamma(\nu)$ functions. These include the mechanical effect of the spatially averaged changes of the magnetic field, as well as the effects of such changes on the convective and thermal structure of the outer layers. These were discussed, e.g., by GMWK and DGS. A full description of all these contributors requires five unknown functions of depth. We note that for the parts of the interior most robustly probed, the $\gamma(\nu)$ from observations are not sufficiently accurate to even think about a formal inversion. All that may be done is to fit simple functional dependences for each specified contributor. This is what we do here, following approaches adopted by GMWK and DGS in their assessments of the field required to explain p -mode frequency changes.

4. VARIATIONAL EXPRESSIONS FOR γ

Hamilton's variational principle is our tool for interpreting the frequency changes. It was employed, for instance, by GMWK and by DG, whose integral formulae linking the γ -values to changes in the magnetic field, turbulent pressure, and temperature are used in the present paper. The approach adopts an adiabatic approximation for oscillations, which may not be fully justified in the part of the outer layers of our interest. DG also provided expressions for calculating frequency splittings represented by the even- a coefficients. Here we give a summary of only the formulae that are relevant for calculating the centroid frequencies.

The underlying variational expression for the angular frequency, $\omega (= 2\pi\nu)$, shift used here is

$$\Delta\omega = \frac{\Delta(D_p + D_M + D_v)}{2I\omega}. \quad (2)$$

The quantities D_p , D_M , and D_v represent contributions of pressure, magnetic field, and turbulent velocity, respectively, to mode frequency. The quantity

$$I = \int d^3x \rho |\xi|^2 = R^5 \bar{\rho} \bar{I} \quad (3)$$

is the mode inertia, and ξ is the Lagrangian displacement vector calculated in a standard spherical model. Here we have ignored terms resulting from changes in gravity and large-scale velocity fields, since both were found to be negligible.

Only the rms values averaged over spherical surfaces contribute to the changes in the mean frequencies, $\bar{\nu}$. The pressure term may be written in the form

$$D_p = \int d^3x p [\mathcal{E} + (\Gamma - 1) |\text{div} \xi|^2], \quad (4)$$

where $\mathcal{E} = \xi_{j;k}^* \xi_{k;j}$ and the semicolon denotes the covariant derivative. The Lagrangian change of D_p , which is calculated with $\delta(\rho d^3x) = 0$, requires evaluation of the pressure and density perturbations, δp and $\delta\rho$, respectively, induced by changes in the magnetic fields and correlated changes in the turbulent velocity. Such changes arise from the magnetic field's inhibit-

ing of convection. For the spherically symmetrical part of perturbation considered here, the density perturbation is not determined by the condition of mechanical equilibrium. Here, following DG, we express $\delta\rho$ in terms of δp and the Lagrangian temperature perturbation, δT . We treat changes in the magnetic field, turbulent velocity, and temperature as independent sources of frequency changes, even though they are physically linked. Modeling the effect of magnetic field on convection is still not well understood, and our approach is to use simple reliable physics to derive helioseismic constraints on advanced models.

Both the magnetic and velocity fields are treated as being statistically random, with the net effect on radial structure resulting from their square averaged components. The vertical component was allowed to be different from the two horizontal components. Thus, the covariance matrix for the magnetic field is written in the following form:

$$\overline{B_i B_j} = \delta_{ij} \left[\delta_{jr} \mathcal{M}^V(r) + \frac{1}{2} \mathcal{M}^H(r) (\delta_{j\theta} + \delta_{j\phi}) \right], \quad (5)$$

where δ_{ij} is the Kronecker symbol. We use an unsubscripted δ to denote the Lagrangian changes in solar depth-dependent parameters, while Δ refers to changes in the global parameters. An analogous form was adopted for the turbulent velocities:

$$\overline{\rho v_i v_j} = \rho \delta_{ij} \left[\delta_{jr} \mathcal{T}^V(r) + \frac{1}{2} \mathcal{T}^H(r) (\delta_{j\theta} + \delta_{j\phi}) \right]. \quad (6)$$

Upon assuming mechanical equilibrium in a thin layer, DG (see also GMWK) calculated the change in pressure, δp , resulting from changes in the random magnetic field ($\delta \mathcal{M}^V$, $\delta \mathcal{M}^H$) and in the random velocities ($\delta \mathcal{T}^V$, $\delta \mathcal{T}^H$). The evaluation of the density change requires consideration of the thermal balance. DG calculated ΔD_p assuming an isothermal response of the layer and separately evaluated the contribution to the γ -values from the temperature change, δT .

The total dynamical effect of the magnetic field change on frequencies consists of ΔD_p calculated with $\delta T = 0$ and

$$\Delta D_M = \frac{1}{4\pi} \Delta \left\{ \int d^3x \left[|(\mathbf{B} \cdot \nabla) \xi|^2 - 2 \text{div} \xi^* \mathbf{B} \cdot (\mathbf{B} \cdot \nabla) \xi + \frac{1}{2} |\mathbf{B}|^2 (\mathcal{E} + |\text{div} \xi|^2) \right] \right\}. \quad (7)$$

These two terms combined in equation (2) lead to the following expression for γ :

$$\gamma_M = \int d \left(\frac{d_{\text{phot}}}{1 \text{ Mm}} \right) \left[K_{M,0}^V \left(\frac{\delta \mathcal{M}^V}{1 \text{ kG}^2} \right) + K_{M,0}^H \left(\frac{\delta \mathcal{M}^H}{1 \text{ kG}^2} \right) \right] \mu\text{Hz}, \quad (8)$$

where d_{phot} denotes the depth beneath the photosphere. The explicit expressions for $K_{M,0}^V$ and $K_{M,0}^H$ in terms of radial eigenfunctions of the mode are given in equation (67) of DG. For the case of f -modes we have $K_{M,0}^V \approx \frac{4}{3} K_{M,0}^H > 0$. For p -modes we have $K_{M,0}^V \gg |K_{M,0}^H|$. Figure 4 shows examples of the kernels,

$$K_{M,0}^i = \frac{1}{3} (K_{M,0}^V + 2K_{M,0}^H),$$

for calculating γ due to isotropic changes in the field.

Comparing the kernels for the two f -modes shown in Figure 4 with the behavior of the $\gamma(\nu)$ shown in Figure 2 (*top*), we conclude

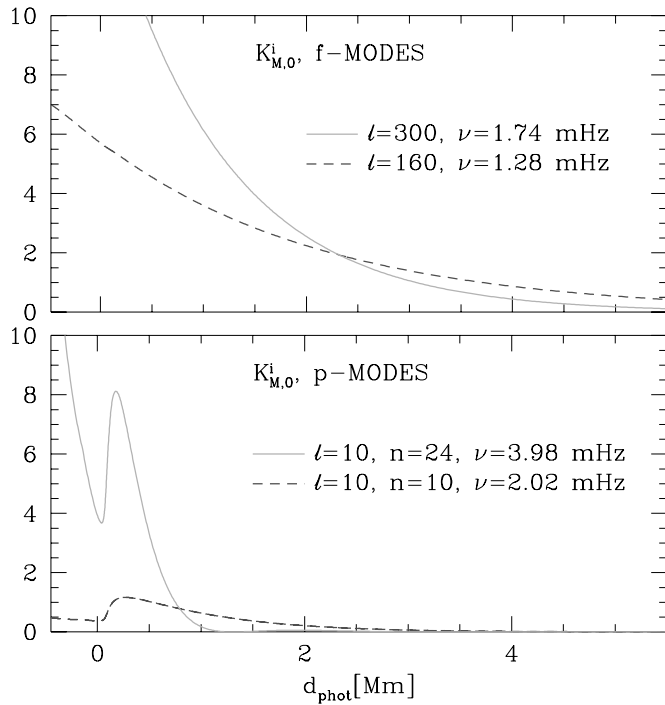


FIG. 4.—Kernels for calculating the γ -values arising from isotropic changes in the magnetic field according to eq. (8), for two selected f -modes (top) and p -modes (bottom) and at two selected frequencies, plotted as functions of depth beneath the photosphere in the outer part of the standard solar models. [See the electronic edition of the Journal for a color version of this figure.]

that if the rise of the magnetic field is responsible for the f -mode γ -values, which decrease between $\nu = 1.28$ and 1.74 mHz, the growth must occur predominantly beneath 2.5 Mm, where the kernel of the lower frequency mode ($\ell = 160$) has higher value.

The kernels for the p -modes plotted in Figure 4 (bottom) were calculated for $\ell = 10$. However, in these outermost layers the kernels of all p -modes in the sample are virtually ℓ -independent. The two kernels have very low values at depths below 2.5 Mm. It is thus clear that the observed p - and f -mode frequency increases cannot be simultaneously explained by an increase in the magnetic field. This conclusion does not depend on the assumed isotropy of the field. Isotropy would have been an essential assumption if the field were the cause of the p -mode frequency rise.

The plots in Figure 5 illustrate the large differences between p - and f -mode kernels at the same frequency. We see that the f -modes in the MDI sample are far more sensitive to magnetic field changes in the outer few megameters beneath the photosphere than the p -modes. We should also note a significant dif-

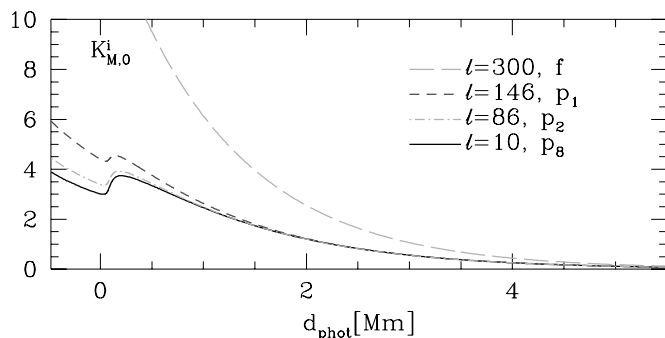


FIG. 5.—Same as Fig. 4, but for modes of nearly the same frequency of $\nu = 1.74$ mHz. [See the electronic edition of the Journal for a color version of this figure.]

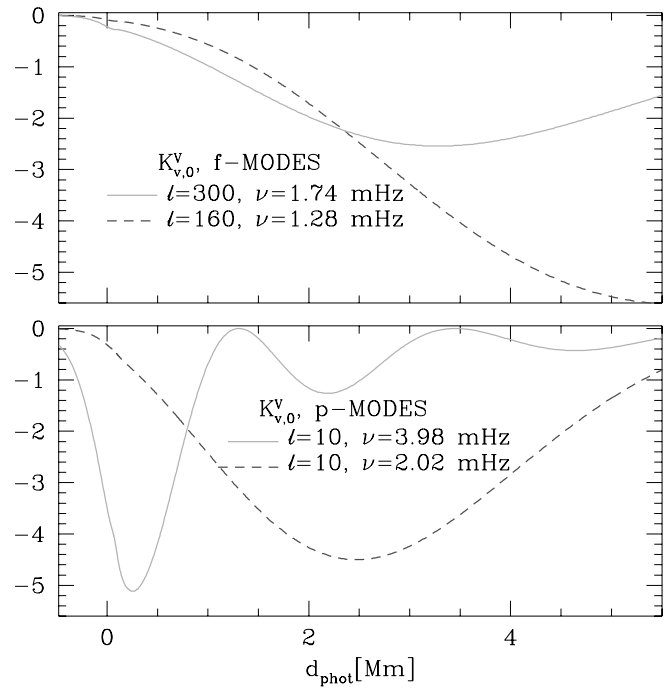


FIG. 6.—Kernels for calculating γ -values arising from the change in the random velocity field according to eq. (10) for two selected f -modes (top) and p -modes (bottom) and at two selected frequencies plotted as functions of depth in the outer part of the standard solar models. [See the electronic edition of the Journal for a color version of this figure.]

ference between p_1 and the higher order p -modes above $d_{\text{phot}} = 1$ Mm. This difference, however, has virtually no consequence because data on p_1 and even p_2 modes are irrelevant for probing this outermost layer.

The overall dynamical effect of the turbulent velocity changes is calculated in a similar way to that for the magnetic field. To the induced change of D_p calculated assuming $\delta T = 0$, we add the change in the velocity term,

$$\Delta D_v = -\Delta \left[\int d^3x \rho |(\mathbf{v} \cdot \nabla) \boldsymbol{\xi}|^2 \right]. \quad (9)$$

When these two terms are used in equation (2), we get, after integration over spherical surfaces,

$$\gamma_v = \int d \left(\frac{d_{\text{phot}}}{1 \text{ Mm}} \right) \times \left[K_v^V \left(\frac{\delta T^V}{1 \text{ km}^2 \text{ s}^{-2}} \right) + K_v^H \left(\frac{\delta T^H}{1 \text{ km}^2 \text{ s}^{-2}} \right) \right] \mu\text{Hz}. \quad (10)$$

Again, we do not give expressions for $K_{v,0}^V$ and $K_{v,0}^H$ here. They were given in equation (59) of DG. In that paper, we plotted the kernels $K_{v,k}^V$ and $K_{v,k}^H$, with $k = 0$ referring to the centroid changes and $k > 1$ to the even- a coefficients. Unfortunately, there was a numerical mistake in those plots. Here we also corrected the error in the previous calculations, reducing the values by a factor of about 9. In Figure 6, we plot corrected kernels for γ due to changes in the vertical component of the velocity for the same four modes that were selected for use in Figure 4. The absolute values of the $K_{v,0}^H$ are smaller (factor $\frac{1}{4}$ for the f -modes, and much less than that for the p -modes). Comparing the plots for the f - and p -modes, we conclude that only in the latter case may one expect a significant effect from changes in the turbulent velocities. The effect should arise mainly above

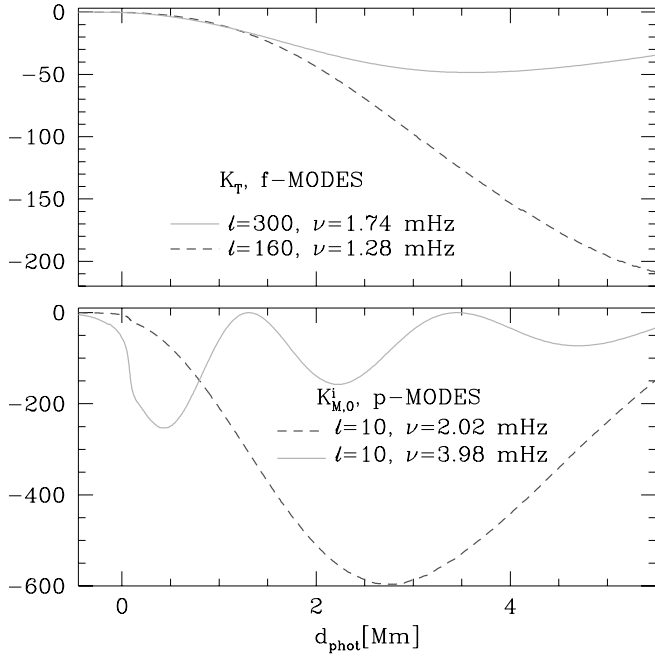


FIG. 7.—Kernels for calculating the frequency shifts due to temperature increase for p -modes at selected frequencies (bottom) and f -mode modes at selected degrees (top). [See the electronic edition of the Journal for a color version of this figure.]

the depth of 1 mM, where the highest velocities are expected. Large effects of turbulence on solar f -modes found in a number of investigations (e.g., Murawski 2000) concerned modes of much higher degrees than considered in this paper.

A decrease in the vertical component of the turbulent velocity remains the most viable explanation of the dominant part of the p -mode frequency increase correlated with the magnetic activity cycle because high-frequency modes preferentially sample the layers where we expect the largest changes in the turbulent velocity. The decrease in the velocities also means a decrease in the efficiency of convective energy transport, hence a decrease of temperature in the outer layers.

As GMWK first observed, an isobaric increase of temperature causes an increase in p -mode frequencies. The same is true for f -modes, but there the effect is much smaller. We express the γ -values due to the Lagrangian change in temperature, δT , in the form

$$\gamma_T = \int d \left(\frac{d_{\text{phot}}}{1 \text{ Mm}} \right) K_T \frac{\delta T}{T} \mu\text{Hz}, \quad (11)$$

again referring readers to DG for an explicit expression for K_T . The plots of K_T for the same four modes as in Figure 6 are given in Figure 7. Here we also decreased the values by a factor of about 9 relative to corresponding plots in DG. The kernels' behavior is similar to that seen in Figure 6. In the shallow sub-photospheric layers, where we may expect the largest relative changes of temperature caused by decreased efficiency of convective transport, only p -modes have substantial amplitudes, and it is only for these modes that a temperature decrease must be considered to be a potentially important contributor to the frequency increase.

5. CHANGES IN SUBPHOTOSPHERIC MAGNETIC FIELD FROM CHANGES IN THE f -MODE FREQUENCIES

The dynamical effect of the rise of the magnetic field seems to be the only possible explanation for the observed f -mode fre-

quency increases. Formally, one can explain the behavior of the $\gamma(\nu)$ values seen in Figure 2 in terms of a decrease in the turbulent velocity, but the decrease would have to be nearly constant with depth, and the amount would have to be unacceptably large at depths greater than, say, 2 Mm.

Probing the depth dependence of the magnetic field based on f -modes has modest precision. Modes in the [180, 300] ℓ -range, for which we have a significant determination of γ , effectively sample the magnetic field down to a depth of only a few (5–6) Mm, but the probing precision is not high because of the spread in the individual frequency shifts.

As a first attempt, we seek the isotropic field change, $\delta(B^2) = \delta(\mathcal{M}^V + \mathcal{M}^H)$, in the form of a truncated power series of the depth below the temperature minimum, $d_{\text{min}} = d_{\text{phot}} + 0.476 \text{ Mm}$,

$$\delta(B^2) = \sum_{k=0} \delta(B^2)_k d_{\text{min}}^k. \quad (12)$$

Including terms up to $k = 2$ enabled us to reach values of χ^2 similar to those of the three-term Legendre polynomial fit of the $\gamma(\nu)$ dependence. The resulting $\delta(B^2)(d_{\text{min}})$ dependence does not look realistic because we found $\delta(B^2) < 0$ near the photosphere (see curves denoted M1 in Fig. 8), as though the near-surface field decreases with rising activity. With this in mind, we tried a form of the $\delta(B^2)(d_{\text{min}})$ function forcing $\delta(B^2) \geq 0$ everywhere. We chose

$$\delta(B^2) = \begin{cases} \delta(B^2)_{\text{int}} & \text{if } d_{\text{min}} \geq d_{\text{int}}, \\ \delta(B^2)_{\text{int}} \left(\frac{d_{\text{min}}}{d_{\text{int}}} \right)^j & \text{if } d_{\text{min}} \leq d_{\text{int}}, \end{cases} \quad (13)$$

with adjustable parameters $\delta(B^2)_{\text{int}}$, d_{int} , and j . The lowest χ^2 of 1.69 was reached at $d_{\text{int}} = 4 \text{ Mm}$ and $j > 20$ (M2 in Fig. 8).

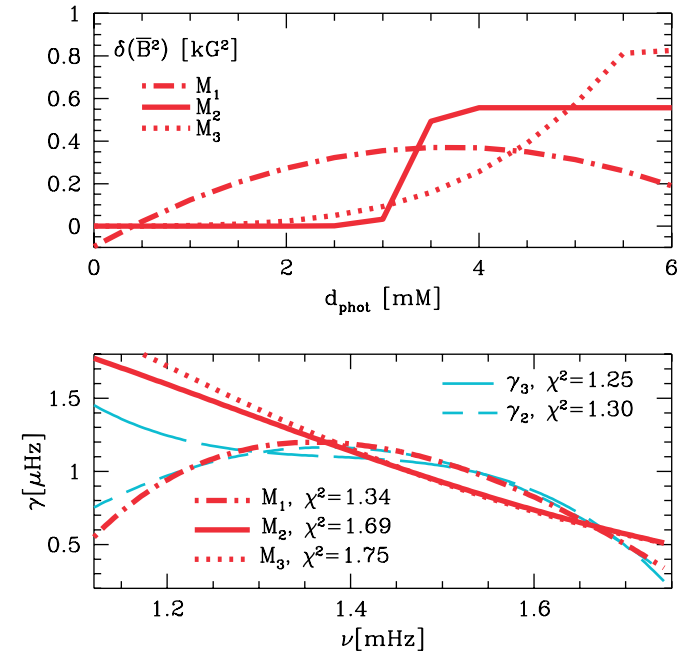


FIG. 8.—Top: Depth dependence of the mean square field change between solar maximum and maximum for models M1, M2, and M3. The errors in individual values of $\delta(B^2)$ for the M1 model are large, growing from 0.03 at $d_{\text{phot}} = 0$ to 0.3 (kG) 2 at $d_{\text{phot}} = 5.5 \text{ Mm}$. Bottom: Bolder lines (red) show the f -mode γ -values calculated for each of the three models. The thinner lines (blue) show $\gamma(\nu)$ functions obtained by fitting truncated Legendre polynomial series as described in § 3.

However, similar values of χ^2 were reached at higher d_{int} and lower j . One such example (M3) is shown in Figure 8.

We see that a concave shape of $\gamma(\nu)$ is reproduced only with the model allowing $\delta(B^2) < 0$, but we do not regard this finding to be significant. Rather, we would blame some inadequacy in our model of the small-scale field in the atmosphere. What we regard as significant is that the f -mode frequency increase between solar minimum and maximum requires both an average field increase of some 0.5–0.7 kG at a depth of about 5 Mm and a much smaller increase close to the photosphere.

6. THE DOMINANT SOURCE OF p -MODE VARIATIONS

Changes in the magnetic fields inferred from f -mode data have only a very small effect on p -mode frequencies. This is illustrated in Figure 9, where in the upper panel we show the seventh-order Legendre polynomial fits of the measured frequency difference after removing the effect of the field according to model M2 (here the choice of the model is not important for our conclusions). Only in the lower frequency regime, below $\nu = 2$ mHz, are the increases in the γ -values with decreasing ν reduced. This suggests that the averaged dynamical effect of the magnetic field rises at a depth of a few megameters and is responsible for an appreciable part of the frequency increase of low-frequency p -modes. However, we should stress that, as we can see in Figure 2, the significance of $\gamma(\nu)$ in this part of the p -mode spectrum is questionable. In any case, most of the p -mode frequency increase with rising activity requires a different explanation.

The high-frequency part of the $\gamma(\nu)$ dependence, which is really significant, may be explained only by invoking an effect acting preferentially close to the Sun's photosphere. The dynamical effect of the growing magnetic field is excluded by measurements of the averaged photospheric field and by the f -mode data. What remains to be considered is an inhibiting effect of the field on convection leading to a lower turbulent velocity and temperature in the outermost layers. The two effects are expected to be significant only close to the photosphere. The question to answer is how much of a reduction is required to account for the observed frequency changes.

We first consider the effect of lowering the turbulent velocity. In fact, only the vertical component of it matters because the horizontal components hardly affect p -mode frequencies. The squared averaged vertical velocity in equation (10) is represented in the form of a truncated power series of the depth beneath the temperature minimum, d_{min} ,

$$\delta(T^V) = \sum_{k=0} \delta(T^V)_k d_{\text{min}}^k. \quad (14)$$

It turned out that it suffices to include terms up to $k = 2$ to fit the measured γ -values with a χ^2 better than that from the seventh-order polynomial $\gamma(\nu)$. The fits are compared in Figure 9 (top).

In Figure 9 (bottom), we show the inferred $\delta(T^V)(d_{\text{phot}})$ dependence with the 1σ error bars from the least-squares fit. The changes required to account for the p -mode frequency rise are naturally higher than those assessed by DG, as the kernels they used were grossly exaggerated (by about a factor of 9 because of an error, which has been fixed here), but the crude estimate made therein results in an error that is smaller than should have been expected. With our present corrected and precise analysis, we get higher numbers, but they are not unreasonably high. The comparison with the model values shows that what is required is less than a 2.5% decrease in T^V . That is less than a 1.3% decrease in

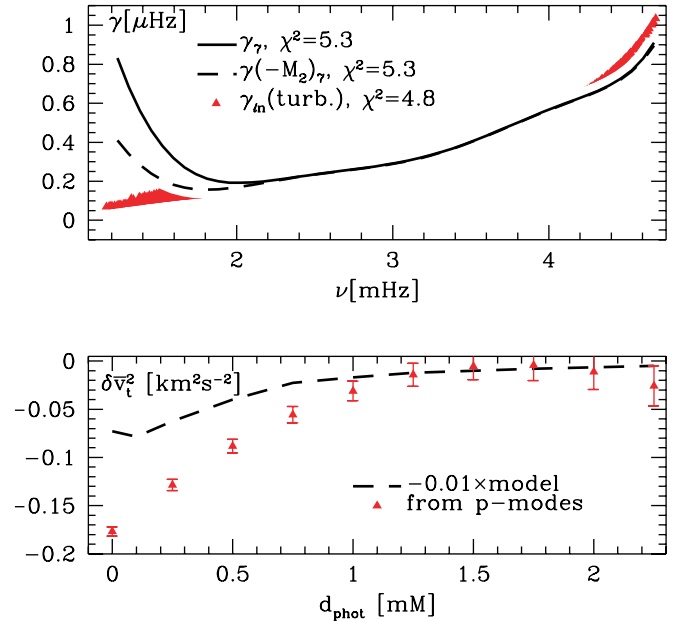


FIG. 9.—Solid and dashed black lines (top) show $\gamma(\nu)$ functions obtained by fitting the Legendre polynomial dependence to measured p -mode frequency shifts before and after removing the effect of magnetic field changes according to model M2 (see Fig. 8, top). Solid red triangles denote individual values of γ_{tn} calculated assuming that the p -mode frequency shift is caused by a decrease in the turbulent velocity. Bottom: Inferred values of the change in the mean squared turbulent velocity compared with the 1% decrease of those values calculated in a model of the solar convective zone of Abbot et al. (1997).

the rms vertical component of the turbulent velocity. We do not believe that this number is in conflict with observations.

A potentially more difficult problem arises from the implications of the reduced convective efficiency on the effective temperature. According to a crude estimate, based on mixing-length approximation and an Eddington atmosphere given by DG, a 1% decrease in the convective velocity is associated with a relative temperature decrease ranging from 1×10^{-3} at $d_{\text{phot}} = 1$ to 3×10^{-3} at $d_{\text{phot}} = 0$ Mm. The values are about one-half of what is needed to account for the p -mode frequency increase by the temperature effect alone. Thus, the required velocity reduction is smaller. Assuming a 0.65% reduction in the rms turbulent velocity and adopting the relation $\delta T_{\text{eff}} \approx \delta T(0)$, we find 8 K for the required decrease in the effective temperature, which seems unacceptably high. Nonetheless, we believe that the inhibiting effect of the magnetic field on convection is the cause of the p -mode frequency increase correlated with increasing activity. We cannot conceive of a more plausible explanation, and we blame the problem regarding the effective temperature change on inadequacies in our treatment of energy transport in the convective zone and in the atmosphere.

7. CONCLUSIONS

We analyzed all available *SOHO* MDI data to study the behavior of the mean solar frequencies with varying magnetic activity. Averaged over their respective frequency ranges, the time variations of p - and f -mode frequencies show the same pattern. Both are strictly correlated with sunspot number. The difference is seen when the mode dependence of the frequency shifts between activity maximum and minimum is compared. The quantities we compare are the shifts scaled by mode inertia, that is, the γ -values. There is a slight residual mode dependence for p -modes, indicating that there is a contribution to the shift arising in deeper layers, but still well above the bottom of the

convective envelope. In the frequency ranges where $\gamma(\nu)$ is well determined, the two types of modes exhibit opposite trends with increasing frequency: growing γ -values for p -modes and declining ones for f -modes. We determined different scenarios as the explanation of the dominant source of the frequency changes in these two cases.

We considered two possible sources of the mean frequency changes: (1) dynamical effects of the changing, average, small-scale magnetic field and (2) effects of turbulent velocity and sub-photospheric temperature changes caused by the impeding effect of the field on convection. In our analysis, we relied on formalism developed by DG. We also corrected a numerical error in estimates presented in that work.

We demonstrated that the main part of the f -mode frequency shifts is explained by the growth of the subphotospheric magnetic field. The relevant growth takes place in the layers at depths of 2.5–5 Mm rising to about 0.5–0.7 kG. The detailed implications regarding both shallower and deeper layers are uncertain beyond the sharp decrease in the field required toward the surface. Formally, the best fit is obtained if there is a slight decrease in the mean photospheric field in the outermost layer with increasing activity, but we do not believe that this is realistic beyond saying the field growth there is small.

Because of its location, the field causing f -mode frequency rise has only a minor effect on p -modes. The weak field rise in the outermost layers is also consistent with the direct measurements of the mean photospheric field (Lin 1995; Lin and Rimmele 1999). This outermost layer is where the dominant source of the frequency p -mode change resides. Thus, we can exclude the field as the source of p -mode changes. Attributing the p -mode frequency shifts to a decrease in turbulence, we found that this requires less than a 2% decrease in the rms value of the vertical component, as calculated in a model of solar convection. Impeded convective flows also cause lower temperatures in the outermost convective layers. Lowering the temperature causes a frequency rise because the effect of cooling is more than compensated by the resulting contraction.

The difficulty of the proposed explanation of the p -mode frequency shifts comes from the implied decrease of the effective temperature by some 8 K between solar minimum and maximum phase. Since our estimate is based on a very crude model, we do not regard this problem as essential, but we think it calls for a

closer study with advanced models of the convective zone and atmosphere of the Sun.

Let us return to the question posed in the title of the DGS paper: *Does the Sun shrink with increasing magnetic activity?* The answer following from our present analysis is yes, it does but not because of the changes at depths beneath 8 Mm, which were previously suggested to lead to shrinking at a rate of about 1.5 km yr⁻¹ during the rising activity phase. The data covering the whole high-activity phase allow a multiple-parameter fit of the frequency change dependence on frequency, $\Delta\nu(\nu)$. We found in § 3 that there is no stable solution for the shrinking rate at the depth of 8 Mm. The dominant effect influencing mass distribution in the outermost layers is the decrease of the turbulent pressure and temperature with increasing activity, and both effects cause shrinking. The implied shrinking amounts to about 1 km between solar minimum and maximum. The roughly 1% decrease of the squared turbulent velocity in the outer 1 Mm below the photosphere must be compensated by a 0.1% density rise because turbulence contributes about 10% of the total pressure. We would obtain the same estimate of the shrinking by attributing part of the p -mode frequency increase to the temperature decrease.

This estimate for the radius change is anticorrelated with activity, and it has the opposite sign from and is much smaller than the change of the photospheric radius derived by Emilio et al. (2000) from the direct measurements based on *SOHO* MDI intensity data. They determined 5.9 ± 0.7 km yr⁻¹ for the rate of the photospheric radius increase during the rise phase of cycle 23. We stress, as in DGS, that the two rates are not directly comparable because the change we derive refers to radius at constant mass and not to constant optical depth.

A cooler and smaller active Sun, whose increased irradiance is totally due to activity-induced corrugation, has been advocated for years by Spruit (e.g., 1991, 2000). Our results support his picture.

This research was supported in part by a Polish grant (KBN-5 P03D 030 20) and US grants from NASA (NAG5-12782 and NNG04GN09G) and NSF (ATM 03-42560). We thank the *SOHO* MDI team, Jesper Schou in particular, for easy access to their fine data.

REFERENCES

- Abbet, W. B., Beaver, M., Davids, B., Georgobiani, D., Rathbin, P., & Stein, R. F. 1997, *ApJ*, 480, 395
- Antia, H. M. 2003, *ApJ*, 590, 567
- Antia, H. M., Basu, S., Pintar, J., & Pohl, B. 2000, *Sol. Phys.*, 192, 459
- Bachmann, K., & Brown, T. 1993, *ApJ*, 411, L45
- Chaplin, W. J., Elsworth, Y., Isaak, G. R., Lines, R., McLeod, C. P., Miller, B. A., & New, R. 1998, *MNRAS*, 300, 1077
- Christensen-Dalsgaard, J., et al. 1996, *Science*, 272, 1286
- Dziembowski, W. A., & Goode, P. R. 2004, *ApJ*, 600, 464 (DG)
- Dziembowski, W. A., Goode, P. R., & Schou, J. 2001, *ApJ*, 553, 897 (DGS)
- Elsworth, Y., Howe, R., Isaak, G. R., McLeod, C. P., Miller, B. A., New, R., Speake, C. C., & Wheeler, S. J. 1994, *ApJ*, 434, 801
- Emilio, M., Kuhn, J. R., Bush, R. I., & Scherrer, P. 2000, *ApJ*, 543, 1007
- Goldreich, P., Murray, N., Willette, G., & Kumar, P. 1991, *ApJ*, 370, 752 (GMWK)
- Kuhn, J. R. 2000, *Space Sci. Rev.*, 94, 177
- Libbrecht, K. G., & Woodard, M. F. 1990, *Nature*, 345, 779
- Lin, H. 1995, *ApJ*, 446, 421
- Lin, H., & Rimmele, T. 1999, *ApJ*, 414, 448
- Murawski, L. 2000, *ApJ*, 537, 495
- Regulo, C., Jimenez, A., Palle, P. L., Perez Hernandez, F., & Roca Cortes, T. 1994, *ApJ*, 434, 384
- Spruit, H. C. 1991, in *The Sun in Time*, ed. C. P. Sonett, M. P. Giampappa, & M. S. Matthews (Tucson: Univ. Arizona Press), 118
- . 2000, *Space Sci. Rev.*, 94, 113
- Woodard, M., Kuhn, J., Murray, N., & Libbrecht, K. 1991, *ApJ*, 373, L81
- Woodard, M., & Noyes, R. 1985, *Nature*, 318, 449